Journal of Soil Science and Plant Nutrition
https://doi.org/10.1007/s42729-024-01935-2

ORIGINAL PAPER

Cascading Effects of Boron Application Methods on Nutrient Distribution and Metabolite Profiles in Pear Trees

Wei Du[1] · Syed Bilal Hussain[2] · Jing Fan[1] · Qiliang Chen[1] · Jingguo Zhang[1] · Xiaoping Yang[1] · Hongju Hu[1,3]

Received: 30 November 2023 / Accepted: 5 July 2024

Abstract
Boron (B) deficiency poses a significant challenge in commercial pear (*Pyrus* spp.) production, typically addressed through root or foliar supply. However, the impact of these B supply methods on plant nutrition and metabolism in pear trees remains relatively unexplored. This study comprehensively examines three B application treatments: control (no B supply), foliar B supply, and root B supply, with B supplied to pear plants in the form of the stable isotope ^{10}B. Both foliar and root B applications increased B concentration and accumulation in various plant tissues, with significant variations in distribution patterns. Notably, foliar application enhanced B accumulation in scion tissues and roots, challenging the traditional limitations of B transport. Furthermore, significant interactions between B application methods and mineral nutrients, particularly nitrogen (N), phosphorus (P), calcium (Ca), and magnesium (Mg), influenced nutrient content and distribution. Metabolite profiling of leaves revealed substantial changes in amino acids, organic acids, and fatty acids in response to B applications, whether foliar or root, suggesting impacts on amino acid metabolism, carbohydrate metabolism, and plant resistance mechanisms. This study highlights the effectiveness of both foliar and root B application methods for B supplementation in pear trees, potentially enhancing growth and stress adaptation. In practical terms, combining foliar and root B applications offers a comprehensive approach to correct B deficiency in pear.

Keywords Boron · Application method · Pear tree · Nutrient content · Metabolite profiles

1 Introduction

Boron (B) is an essential micronutrient for optimal plant growth, reproductive development, and overall performance (Matthes et al. 2020). Its significance extends to various cellular processes, including maintaining cell wall integrity, cytomembrane functionality, metabolite synthesis, carbohydrate transport, and meristem division (Landi et al. 2019; Pereira et al. 2021; Shireen et al. 2018). B deficiency severely impacts plant development, halts root elongation, disrupts apex development, diminishes leaf expansion, and impedes bud differentiation (Archana and Pandey 2021; Wang et al. 2015). To address B deficiency, direct soil application and foliar application are common approaches, with the latter being particularly effective when root absorption capacity is limited (Fernández and Eichert 2009; Kohli et al. 2023).

However, the precise impacts of exogenous B supply on B states within plants, as well as its influence on the absorption and utilization of other essential mineral nutrients in different plant tissues, remain not fully elucidated (Shireen et al. 2018). For instance, B-deficient soybean plants exhibit reduced leaf calcium (Ca) content, lower seed potassium (K) content, and diminished sulfur (S) content in seeds and roots (Pawlowski et al. 2019). Conversely, citrus seedlings subjected to B fertilization experience increases in leaf Ca, magnesium (Mg), phosphorus (P), and zinc (Zn) content, as

Wei Du and Syed Bilal Hussain co-first authors contributed equally to this work.

✉ Xiaoping Yang
yangxiaoping1981@163.com

✉ Hongju Hu
huhongju@hbaas.com

[1] Hubei Key Laboratory of Germplasm Innovation and Utilization of Fruit Trees, Research Institute of Fruit and Tea, Hubei Academy of Agricultural Science, Wuhan, Hubei 430064, P. R. China

[2] School of Agriculture and Food Science, University College Dublin, Dublin 4, Ireland

[3] Hubei Hongshan Laboratory, Wuhan 430070, China

Published online: 15 July 2024

well as heightened Mg, P, K, and Zn levels in roots (Zhou et al. 2014). Comparable trends occur in cotton plants, where soil-applied B enhances nutrient uptake and translocation, influencing nitrogen (N), P, K, Zn, and iron (Fe) distribution across leaves, buds, and seeds (López-Lefebre et al. 2002). In addition to influencing plant mineral nutrient status, B application triggers metabolic alterations, affecting amino acid metabolism, carbohydrate processes, and membrane transport (Gao and Chao 2022; García-Sánchez et al. 2020; Lu et al. 2014; Wang et al. 2022). Given B's ability to modulate plant mineral nutrient status, changes in B availability may exert regulatory control over metabolic processes by influencing the tissue content of other essential nutrient elements. For instance, N influences amino acid metabolism (Tegeder and Hammes 2018). P regulates acid metabolism and indirectly contributes to carbohydrate synthesis and breakdown (Lu et al. 2014; Luo et al. 2019; Wang et al. 2023). Mg is a structural component of chlorophyll, impacting photosynthetic efficiency (Tian et al. 2021).

Pear is one of the most important cultivated fruit trees worldwide, with numerous varieties intolerant to B deficiency, resulting in yield and quality losses (Liu et al. 2023; Silva et al. 2014; Xuan et al. 2005). Unlike evergreen trees, deciduous pear trees rarely exhibit visible leaf symptoms due to leaf shedding after harvest (Jiang et al. 2020). B deficiency symptoms manifest in buds and fruit as wizened buds and cork spot symptoms (Du et al. 2022; Zhang et al. 2023), indicating structural impairment in pear plant reproductive organs. Despite subsequent B supplementation, symptoms persist (Wang et al. 2015), highlighting the need for further investigation into B fertilization efficiency.

In pear cultivation, both foliar and soil-based B applications are commonly used for supplementation. However, the impact of these methods on B distribution, utilization, and their potential influence on other mineral nutrients and metabolic processes are not yet fully understood. This study aims to investigate how foliar and soil-based B application methods in pear trees influence B distribution, utilization, and their potential interactions with other mineral nutrients and metabolic processes.

2 Materials and Methods

2.1 Plant Materials, Treatments, and Sampling

One-year-old 'Jindai' pear (*Pyrus pyrifolia*) plants, grafted onto Callery pear (*P. calleryana*) rootstocks, were individually planted in 5-L lightproof pots containing a B-free culture medium (quartz sand: perlite: vermiculite = 1:1:1). All grafted plants were cultivated in a greenhouse (average temperature≈33℃, average relative humidity≈80%) at the Hubei Academy of Agricultural Science, Research Institute of Fruit and Tea, in Wuhan, China. Before initiating treatments, each grafted plant received 1 L of modified Hoagland No. 2 nutrient solution without B (composition: 6 mM KNO_3, 4 mM $Ca(NO_3)_2$, 1 mM $NH_4H_2PO_4$, 2 mM $MgSO_4$, 9 μM $MnCl_2$, 0.8 μM $ZnSO_4$, 0.3 μM $CuSO_4$, 0.01 μM H_2MoO_4, and 50 μM Fe-EDTA) (Hoagland and Arnon, 1950) every 3 days for a span of 2 weeks. This allowed the plants to adapt to the sand culture conditions. Subsequently, plants with comparable stem diameter, plant height, and vigor were selected for three distinct treatments: T1—control, where leaves were wiped with ultra-pure water and the root was supplied nutrient solution without B; T2—leaves were wiped with a 0.2% solution of ^{10}B ($H_3{}^{10}BO_3$, 99% purity, Aldrich) once in the first week and then, the root was supplied with a nutrient solution (Hoagland No. 2 nutrient solution without B) every 3 days; T3—leaves were wiped with ultra-pure water and the root was supplied with sufficient ^{10}B (0.25 mg L^{-1}, $H_3{}^{10}BO_3$, 99% purity, Aldrich) and a nutrient solution (Hoagland No. 2 nutrient solution without B) every 3 days. Each treatment was replicated four times with one plant as one replication. Any damaged leaves and leaves unsuitable for treatment were removed, retaining 10–13 healthy leaves on each treated plant.

50 days after treatment initiation, leaves, buds, stems, and roots of the treated plants were collected separately. Following a double wash in distilled water, a portion of fresh leaves was oven-dried for nutrient analyses. Other fresh leaves were flash-frozen with liquid nitrogen and stored in an ultra-low-temperature freezer (-80 °C) for metabolite analyses and nitrogen content detection.

2.2 Determination of Ionome

For N concentration measurement, fresh samples of various tissues weighing 0.2–1.0 g were analyzed using a Vario MACRO Cube Analyzer (Elementar, Germany) (Tian et al. 2022). Additionally, dry samples of different tissues weighing 0.3–1.0 g were ashed in a muffle furnace at 500 °C for 6 h and then dissolved in a 1% HNO_3 solution (20 mL). Half of the solution was utilized to quantify the concentrations of B (natural abundance), P, K, Ca, Mg, S, Fe, manganese (Mn), copper (Cu), and Zn using an inductively coupled plasma-optical emission spectrometer (ICP-OES, Finnigan MAT, Element I, Germany).

Nutrient accumulation (μg) was calculated as Nutrition concentration (μg g^{-1}) × Dry weight (g), and nutrient distribution (%) was calculated as Nutrient accumulation (μg) / Total nutrient content (μg $plant^{-1}$).

2.3 Determination of ^{10}B Proportion

The remaining half of the dissolved solution was employed to determine the abundance (%) of ^{10}B in plant tissues via an

inductively coupled plasma-mass spectrometer (ICP-MS) at the Institute of Soil Science, Chinese Academy of Sciences. With the natural abundance of ^{10}B in natural boron and supplied $H_3{}^{10}BO_3$ being 20 ± 0.02% and 99%, respectively, the ^{10}B proportion (derived from treatments) was calculated using the formula:

^{10}B proportion (%) = (^{10}B abundance (%)—20%) / (99%—20%) × 100%.

2.4 Sample Preparation for Metabolome Detection

Leaf samples (approximately 1–2 g) were weighed and ground in 2 mL Eppendorf tubes with a 5 mm tungsten bead for 1 min at 65 Hz in a grinding mill prior to metabolite extraction. Metabolites were extracted using a pre-cooled mixture of methanol, acetonitrile, and water (v:v:v, 2:2:1), followed by 1 h of ultrasonic shaking in ice baths. The mixture was then cooled at -20 °C for 1 h and subsequently centrifuged for 20 min (14,000 g, 4 °C). Supernatants were collected and concentrated to dryness in a vacuum.

2.5 UHPLC-MS/MS Analysis

Metabolomics profiling was performed using a UPLC-ESI-Q-TOF–MS system (UHPLC, 1290 Infinity LC, Agilent Technologies, Santa Clara, CA, USA) coupled with Triple TOF 5600 (AB Sciex, Framingham, MA, USA). For hydrophilic interaction liquid chromatography (HILIC) separation, samples were analyzed on a 2.1 mm × 100 mm ACQUITY UPLC BEH Amide 1.7 µm column (Waters, Ireland). Both electrospray ionization (ESI) positive and negative modes were used for MS data acquisition. To ensure data normalization, quality control samples and blank samples (75% acetonitrile) were prepared by pooling aliquots of all samples and injected every six samples during acquisition. Detailed conditions for HILIC separation and MS data acquisition are described in the Supplementary Methods.

2.6 Metabolic Data Analysis

The MS data underwent processing using XCMS for feature detection, retention time correction, and alignment. Metabolite data were matched against a standards database. Multivariate statistical analysis employed SIMCAP software (Version 14.0, Umetrics, Sweden). The overfitting Partial Least-Square Discriminant Analysis (OPLS-DA) model was constructed using permutation tests. Differential metabolites were identified based on the Variable Importance on Projection (VIP) score from the OPLS-DA model. To elucidate perturbed biological pathways, differential metabolite data underwent KEGG pathway analysis utilizing the KEGG database (http://www.kegg.jp). Further details on OPLS-DA modeling, VIP score calculation, and KEGG pathway enrichment analysis are available in the Supplementary Methods.

2.7 Determination of Organic Acids and Amino Acids

For extraction, 500 µL of 10% formic acid in methanol–water (1:1, v/v) was used along with 100 mg of glass beads, followed by vortexing for 60 s. After grinding, all samples were centrifuged (12,000 rpm, 4 °C, 10 min), and 10% formic acid in methanol–water (1:1, v/v) was added again at a 50-fold dilution. The resulting supernatant was filtered through a 0.22 µm membrane, and the filtrate was transferred to the LC–MS vial. Organic acids and amino acids concentration were determined using UHPLC-MS (ACQUITY Liquid chromatography coupled with AB5000 MS, Waters and AB SCIEX, USA). The concentration of the test samples was calculated using the standard curve derived from standard sample testing. More detailed methods for the determination of organic acids and amino acids are provided in the Supplementary Methods.

2.8 Statistical Analysis

Unless explicitly stated, all values were expressed as means ± standard deviation (SD) of 4 replications. Comparison analysis was performed using ANOVA (Duncan test, $P < 0.05$) in SPSS for Windows 19.0 (SPSS Inc., Chicago, IL, USA). Principal Component Analysis (PCA) and correlation analysis (Pearson, $P < 0.05$) were conducted using online software (Metaware Cloud).

3 Results

3.1 B Concentration, Accumulation, Distribution and ^{10}B Proportion in Various Tissues of B Treated Plants

The B concentration was assessed to determine the impact of different B treatments on tissue B content (Fig. 1A and Table S1). The B concentration exhibited distinct profiles across various tissues. In leaves, T2 had the highest B concentration, followed by T3, and T1 had the lowest concentration (Fig. 1A and B). Similar trends were observed in buds and stems, with T2 showing a higher B concentration than T1 and T3, while T1 had a lower concentration than T3 (Fig. 1A and B). In roots, T3 had a significantly higher B concentration than T1 and T2, with T2 also having a higher concentration than T1 (Fig. 1A and B).

B distribution was calculated to investigate changes in distribution capacity resulting from different B applications. A significantly higher B distribution was observed in the roots

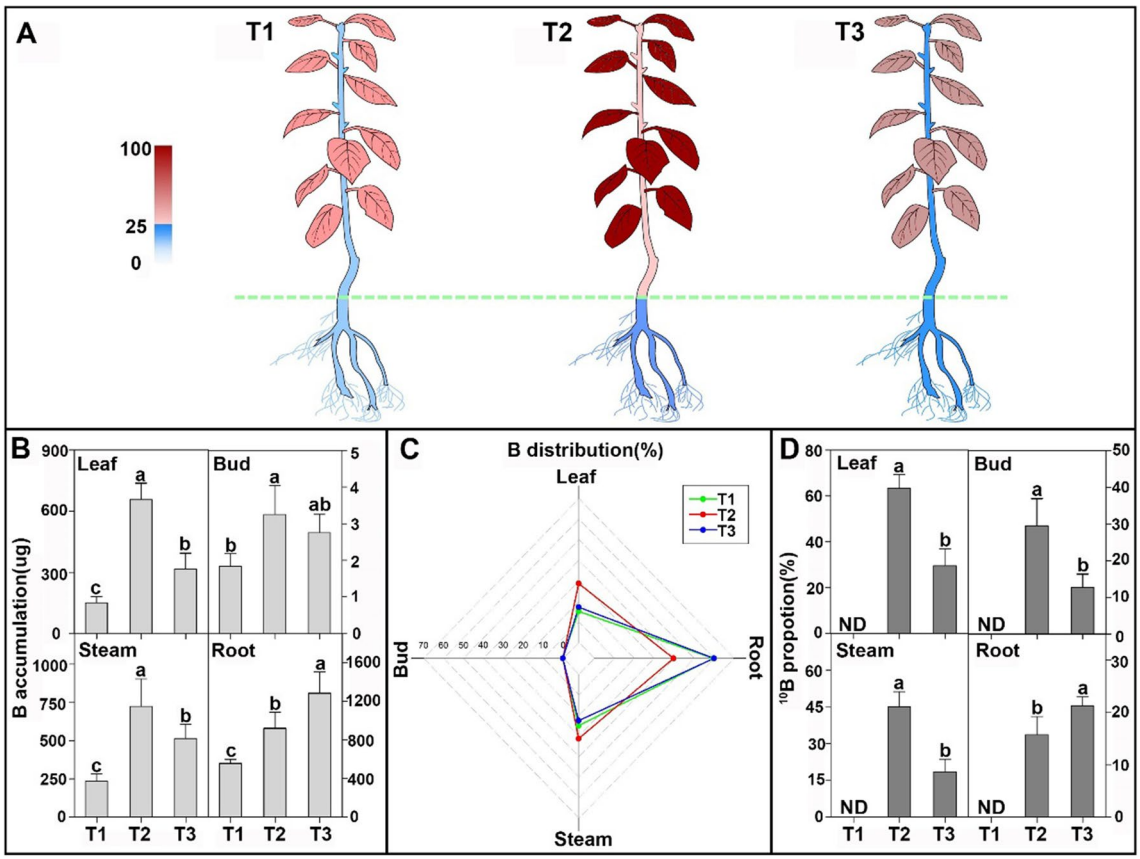

Fig. 1 Comparison of Boron Concentration (**A**), Boron Accumulation (**B**), Boron Distribution (**C**), and ^{10}Boron Proportion (**D**) in Different Tissues of T1-T3 Treated Pear Plants. T1: control without boron supply; T2: foliar boron supply; T3: root boron supply. The color gradient in graph A from white to blue represents a boron concentration range of 0–25 mg kg^{-1}, while the shades from light red to dark red indicate a concentration range of 25–100 mg kg^{-1} of boron in various tissues. 'ND' indicates no detection. Different lowercase letters in each graph indicate significant differences among treatments at $P < 0.05$ using the Duncan test

of T1 and T3 compared to T2 (Fig. 1C). However, leaves and stems in T1 and T3 showed a 20%-47% reduction in B distribution compared to T2 (Fig. 1C). Notably, no significant difference in B distribution was found in bud tissues (Fig. 1C).

Furthermore, the ^{10}B proportion was evaluated following varied B applications to analyze the uptake of newly absorbed B from the solution. Figure 1D showed that the ^{10}B proportion was significantly higher in leaves, buds, and stems of T2 compared to T3, whereas in roots, T3 displayed a significantly higher proportion of ^{10}B than T2. Remarkably, the trend in ^{10}B proportion aligns with the B concentration comparison between T2 and T3 (Fig. 1A and D). As expected, no ^{10}B proportion was detected in T1 tissues since they did not receive any ^{10}B supply.

3.2 Concentration and Distribution of Other Mineral Nutrients in Different Tissues of Different Treated Plants

The ionic data underwent PCA analysis, and the significant differences among T1-T3 treatments in different tissues were revealed through the PCA score plot (Fig. 2). The primary components of PCA, PC1 and PC2, accounted for 98.86% and 0.63%, 98.45% and 0.82%, 97.72% and 1.73%, 96.11% and 2.13% of the overall variance in leaves, buds, stems, and roots, respectively. These principal components effectively elucidated mineral nutrient changes in response to various B applications across different tissues. Notably, examination of PC1 and PC2 highlighted that the mineral nutrients N, Mg,

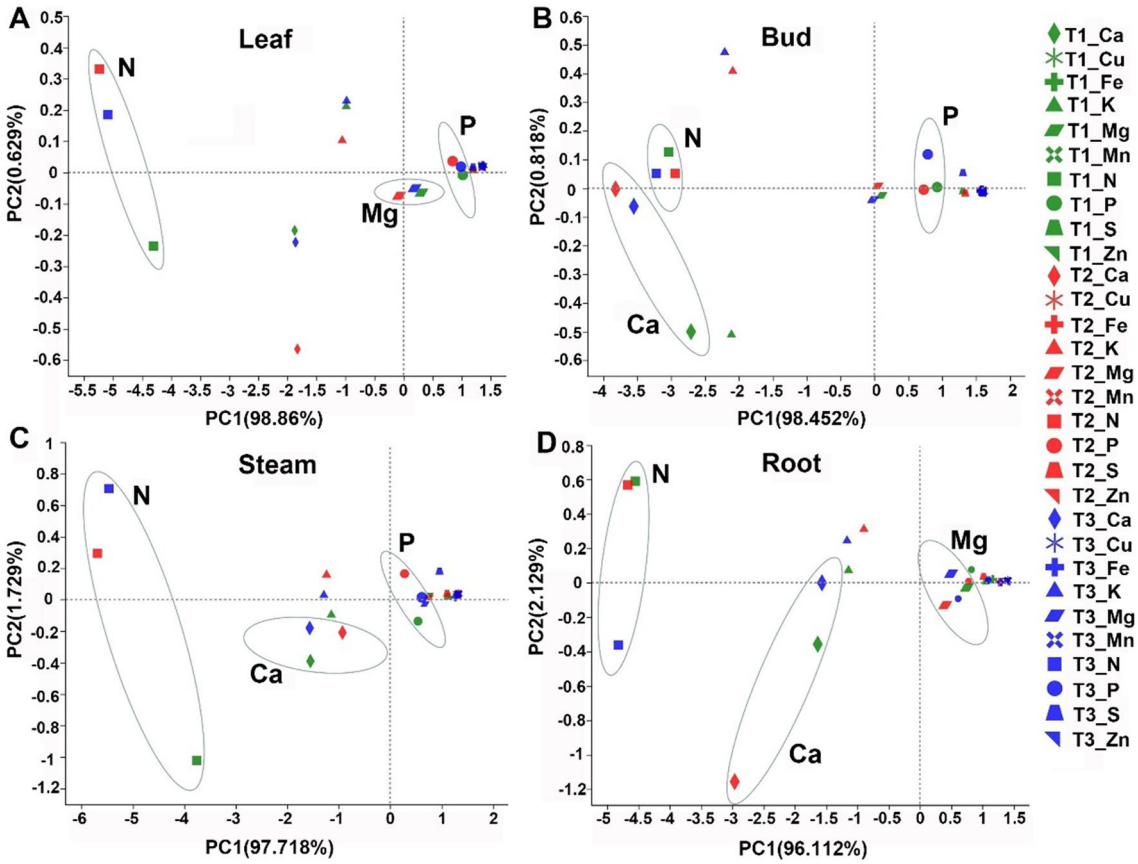

Fig. 2 Principal Component Analysis (PCA) of Mineral Nutrients in Leaf (**A**), Bud (**B**), Stem (**C**), and Root (**D**) of T1-T3 Treated Pear Plants. The three circles within each graph represent the three most distinct mineral elements (same shape of legends) of T1-T3 treated pear plants (same color of legends), respectively. T1: control without boron supply; T2: foliar boron supply; T3: root boron supply. PC: principal component. N: nitrogen. P: phosphorus. Ca: calcium. Mg: magnesium

and P in leaves (Fig. 2A), N, Ca, and P in buds (Fig. 2B), N, Ca, and P in stems (Fig. 2C), and N, Ca, and Mg in roots (Fig. 2D) significantly contributed to the main separation, representing the three most distinctive mineral nutrients in each tissue.

Guided by the PCA analysis, N, P, Ca, and Mg, which exerted a dominant influence under different B applications, were selected for further investigation of nutrient concentration and distribution. As shown in Fig. 3A, the N concentration in leaves and stems of T2 and T3 was significantly higher than in T1. Furthermore, T1-T3 treatments displayed similar N distribution patterns, with T2 exhibiting approximately 28% higher leaf N distribution and 18% higher stem N distribution than T1 and T3.

Regarding P (Fig. 3B), the P concentration in leaves and stems of T2 was notably higher than that in T1 and T3. Conversely, the P concentration in roots of T3 surpassed that in T1 and T2. Within the root tissues of T1-T3 treatments, T3 exhibited the highest P distribution, while T2 had the lowest. In contrast, T2 displayed the highest stem P distribution, whereas T3 had the lowest. Moreover, T2 exhibited approximately 60% and 73% higher P distribution than T1 and T3, respectively.

Concerning Ca (Fig. 3C), the Ca concentration in buds of T2 was significantly higher than in T1. In stems, the Ca concentration of T2 was significantly lower than in T1 and T3. However, in roots, the Ca concentration was significantly higher in T2 compared to T1 and T3. The distribution of Ca differed significantly in roots and stems among T1-T3. Specifically, the root Ca distribution of T2 was about 10% higher than T1 and approximately 56% lower than T3.

For Mg (Fig. 3D), significant variations in Mg distribution were evident among T1-T3 treatments in leaves and roots. The highest Mg distribution in leaves occurred in T2, followed by T3, and the lowest in T1. Additionally, the Mg concentration in roots of T1 was considerably lower than that in T2 and T3. Notably, the most notable differences in Mg distribution were observed in leaf and stem tissues. The Mg distribution in T2 leaves was approximately 28% higher than in T1 and T3, whereas the Mg distribution in T1 stem exceeded that in T2 and T3 by approximately 55% and 33%, respectively.

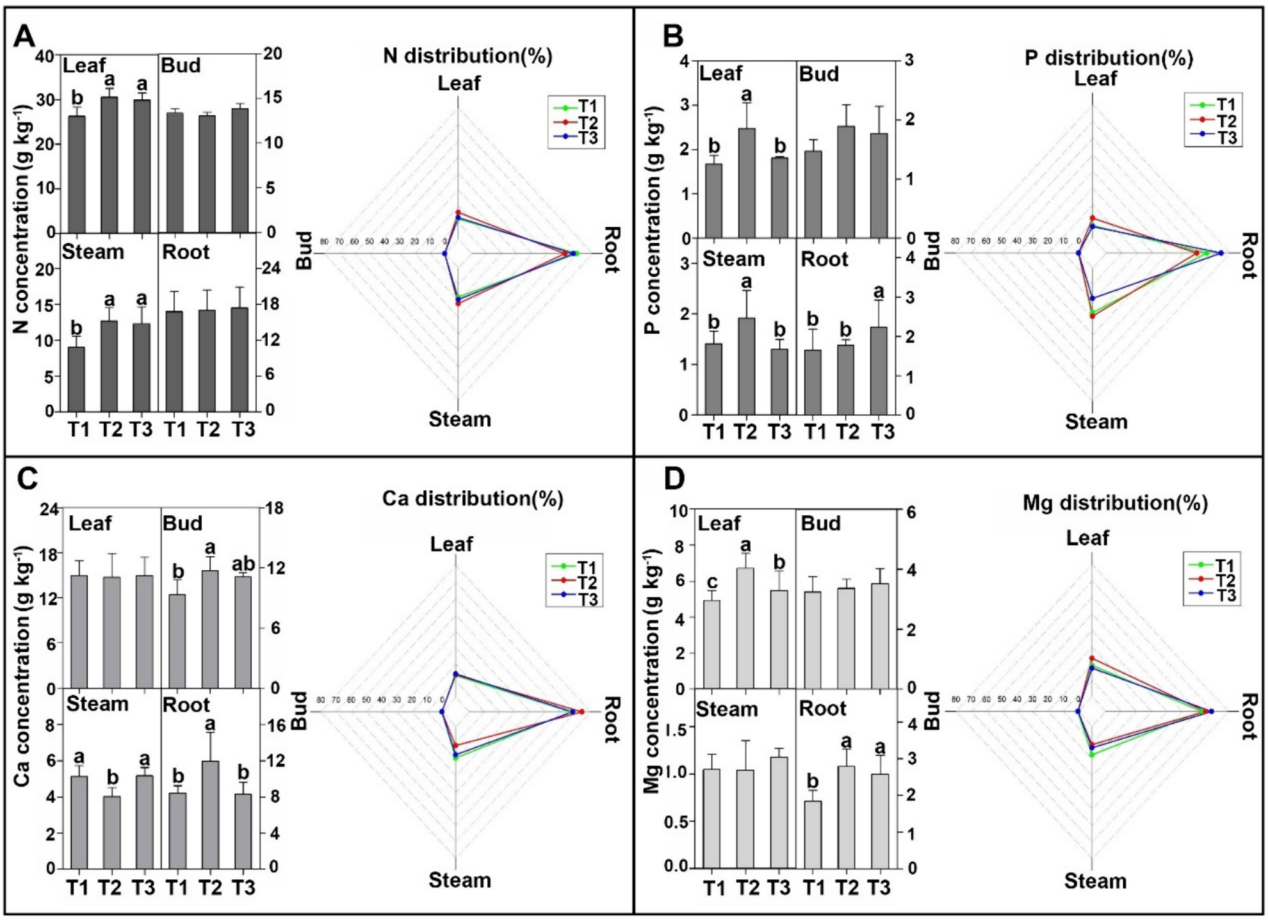

Fig. 3 Comparison of Concentration and Distribution of Nitrogen (**A**), Phosphorus (**B**), Calcium (**C**), and Magnesium (**D**) in Different Tissues of T1-T3 Treated Pear Plants. Different lowercase letters in each graph indicate significant differences among treatments at $P < 0.05$ using the Duncan test. T1: control without boron supply; T2: foliar boron supply; T3: root boron supply. N: nitrogen. P: phosphorus. Ca: calcium. Mg: magnesium

3.3 Metabolite Changes in Leaves of Different Treated Plants

OPLS-DA score plots were employed to effectively differentiate the sample groups by maximizing covariance between the leaf data sets of T1, T2, and/or T1, T3 (variable X). The initial components within the OPLS-DA score plots distinctly demonstrated the separation between T1 and T2 (Fig. 4A), as well as T1 and T3 (Fig. 4B), with an explanatory power of 0.61 (R2X) for X variation within the leaves of T1 and T2, and 0.45 (R2X) for X variation within the leaves of T1 and T3. These results highlighted the potential for further metabolite analysis of leaves within the context of treatment separation.

In leaves, a total of 422 differential metabolites (between T1 and T2) or 232 (between T1 and T3) were identified, with 256 (between T1 and T2) or 92 (between T1 and T3) down-regulated metabolites and 166 (between T1 and T2) or 140 (between T1 and T3) up-regulated metabolites (Fig. 5A, C). Before investigating the correlation between differential metabolites and mineral nutrients, metabolic profiling (based on VIP score) was conducted to pinpoint the key differential metabolites among treatments. Five classes of metabolites were scrutinized within the analysis of leaf differential metabolites between T1 and T2 or T1 and T3 (Fig. S1). Specifically, Fig.S1A highlighted 44 leaf metabolites classified as amino acids (AA), fatty acids (FA), organic acids (OA), steroidal saponins (SS), and triterpenoids (TP), collectively constituting over 10% of the total number of differential metabolites between T1 and T2. Furthermore, Fig. S1B revealed 35 leaf metabolites categorized as AA, FA, OA, TP, and limonoids (LM), encompassing over 15% of the differential metabolites between T1 and T3. Within these five classes of differential leaf metabolites, 11 AA, 4 FA, 3 OA, 8 SS, and 7 TP were up-regulated, whereas 4 FA, 4 OA, 1 SS, and 2 TP were down-regulated when comparing T1 and T2 (Fig. 5B). Similarly, in the comparison of T3 with T1, 6 AA, 4 FA, 3 OA, 2 SS, and 7 TP were up-regulated, while

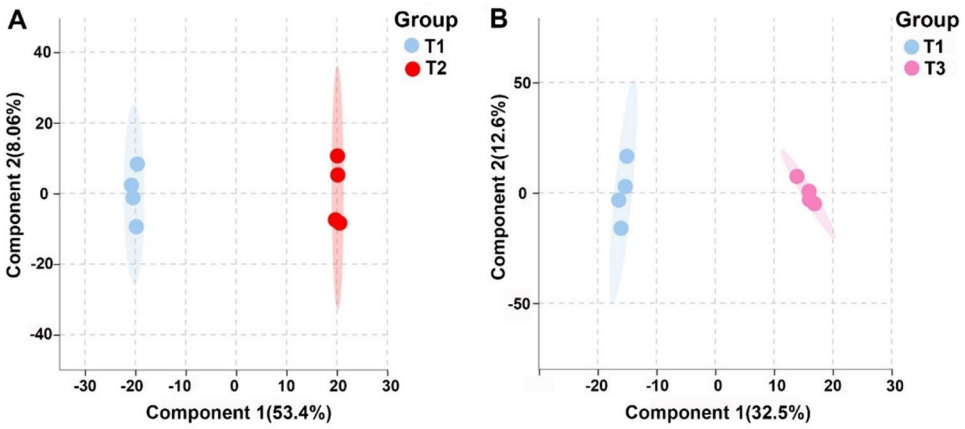

Fig. 4 OPLS-DA Score Plots of Leaf Samples Derived from UPLC-ESI-Q-TOF–MS Spectra for the Comparison of T1 and T2 Treatments (**A**), and T1 and T3 Treatments (**B**). T1: control without boron supply; T2: foliar boron supply; T3: root boron supply

2 AA, 3 FA, 2 OA, 4 SS, and 2 TP were down-regulated in leaves (Fig. 5D).

3.4 Correlations Between Differential Metabolites and/or KEGG

Further correlation analyses were undertaken to elucidate the intrinsic relationships between mineral nutrients and differential metabolites in leaves. Significant correlations emerged between 14 metabolites and B, N, P, Mg in the leaves of T2, and 12 metabolites and B, N, P, Mg in the leaves of T3, respectively (Fig. S2). Specifically, Fig. S2A revealed that AA, FA, OA, TP, and 2 steroidal saponins (SA) exhibited significant correlations with mineral nutrients in the leaves of T2. Furthermore, Fig. S2B depicted that 5 AA, 1 FA, 3 OA, 4 TP, and LM displayed significant correlations with the altered nutrient concentration in the leaves of T3 (detailed positive and negative correlations between specific metabolites and mineral nutrients were presented in Fig. S2).

Beyond the content correlation between mineral nutrients and metabolites, significant changes were observed within metabolic pathways corresponding to the altered mineral nutrient content in the leaves. KEGG analysis of leaf metabolites identified 8 identical pathways derived from the top 20 KEGG pathways (ranked by p-value) that were consistent in both the T1-T2 (Fig. 6A) and T1-T3 (Fig. 6B) comparisons. These 8 pathways were classified into 4 categories: amino acid metabolism, carbohydrate metabolism, membrane transport, and metabolism of cofactors and vitamins (Fig. 6).

3.5 Organic Acids and Amino Acid Concentration in Leaves of Different B Supply

KEGG analysis revealed the tricarboxylic acid (TCA) cycle, a pivotal component of carbohydrate metabolism, to be prominently influenced by the differential metabolite profiles in leaves under varied B-supply treatments. Among the TCA cycle-associated organic acids, the concentrations of citrate and succinate were notably elevated in the leaves of both T2 and T3 in comparison to T1 (Fig. 7A). Interestingly, succinate concentration was markedly higher in T2 than T3, while the concentrations of fumarate and malate were consistently lower in T2 compared to T3 (Fig. 7A).

Analysis of amino acids involved in the TCA cycle revealed distinct trends. Concentrations of glutamate, glutamine, histidine, aspartate, asparagine, threonine, and GABA were markedly lower in the leaves of T1 compared to both T2 and T3 (Fig. 7B). Methionine and ornithine concentrations were exclusively lower in T1 compared to T2, with no difference observed between T1 and T3 (Fig. 7B). Interestingly, proline concentration displayed a significantly higher level in T1 compared to T3. With the exception of glutamine (wherein no difference was observed between T2 and T3), the remaining 9 amino acids consistently exhibited higher concentrations in T2 leaves relative to T3 (Figs. 7B and 8).

4 Discussion

B deficiency is a widespread issue in fruit production, commonly addressed through soil or foliar B application (Al-Obeed et al. 2018; Shireen et al. 2018). Our research confirms the effectiveness of both foliar and root B applications in rectifying B deficiency, enhancing B concentrations, and promoting growth in leaves, stems, and roots of pear plants. Notably, leaf tissues exhibited higher B concentrations and ^{10}B proportions across both treatments, suggesting a preference for B allocation to leaves during the vegetative phase in pear trees.

The absorption of B from soil occurs through roots, which is then transported via xylem to support plant growth (Bolan et al. 2023; Chen et al. 2023). However, when root-absorbed B falls short of plant demands, foliar B application offers a rapid corrective approach (Fernández and Eichert 2009; Mahendran et al. 2022). In our study, both foliar and root B

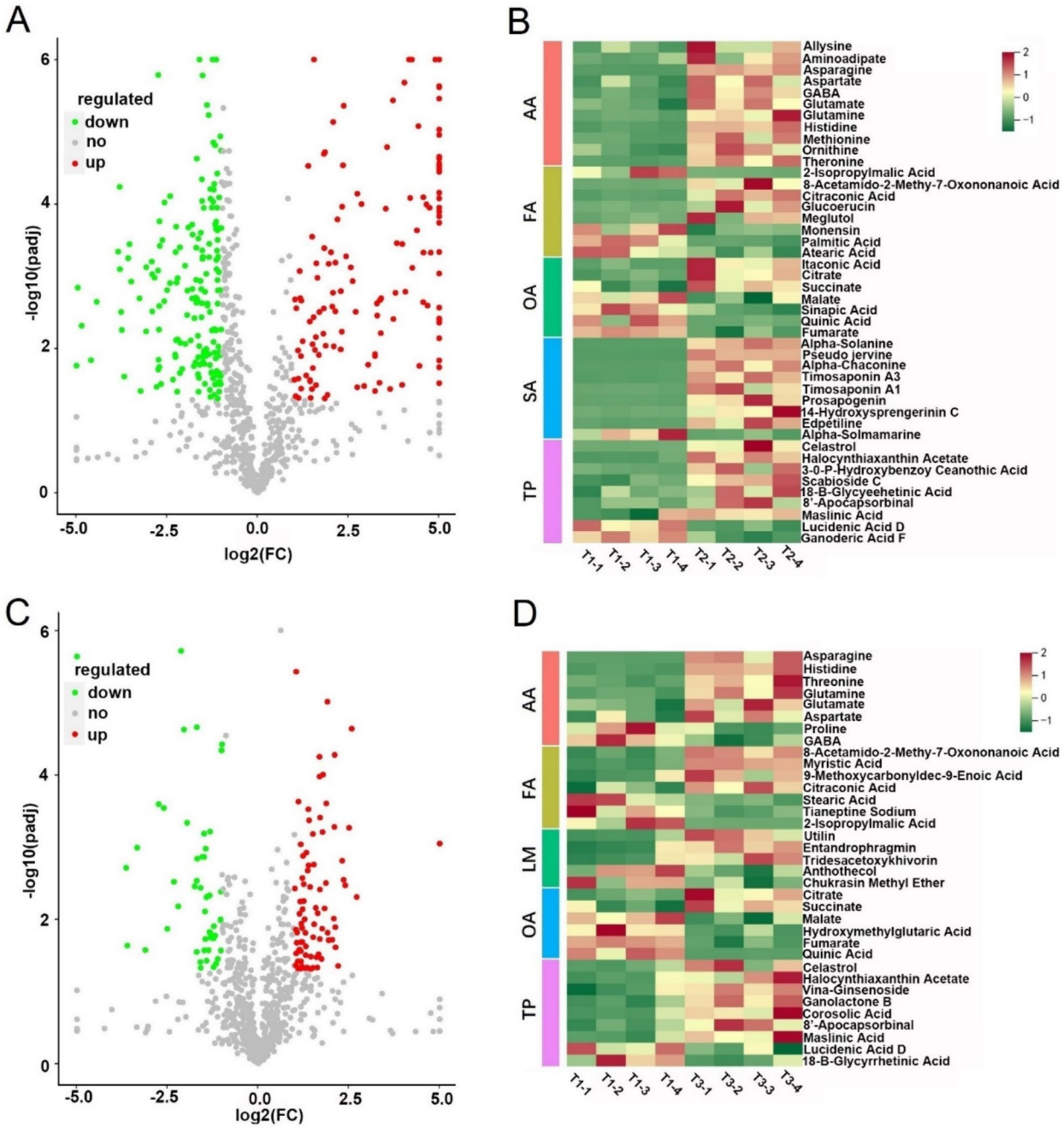

Fig. 5 Differential Metabolite Analysis in Leaves of Treated Pear Plants. **A**, **C** Volcano Maps; **B**, **D** Heat Maps. Metabolites were compared between T1 and T2 treatments (**A**, **B**) or T1 and T3 treatments (**C**, **D**), respectively. The color gradient in graph B and D from green to red represents log2 (fold changes). T1: control without boron supply; T2: foliar boron supply; T3: root boron supply. AA: amino acids. FA: fatty acids. OA: organic acids. SS: steroidal saponins. LM: limonoids. TP: triterpenoids. FC: fold change

applications resulted in higher B accumulation in specific tissues, facilitating a consistent nutrient supply from sources to sinks through both methods. Notably, foliar B application led to enhanced B accumulation in roots after being transported from leaves, contradicting concerns of B transport limitations. This effect may be attributed to pear plants' robust B mobility, facilitated by cis-diols like sorbitol that form borate-sorbitol complexes (Bairu et al. 2009; Brown and Hu 1996), suggesting that foliar application could comprehensively improve B status in pear plants.

B absorption exhibits variations between foliar and soil applications, resulting in distinct distribution patterns of B (Zhao and Oosterhuis 2002). Our findings indicate significantly higher B concentration, B accumulation, and a

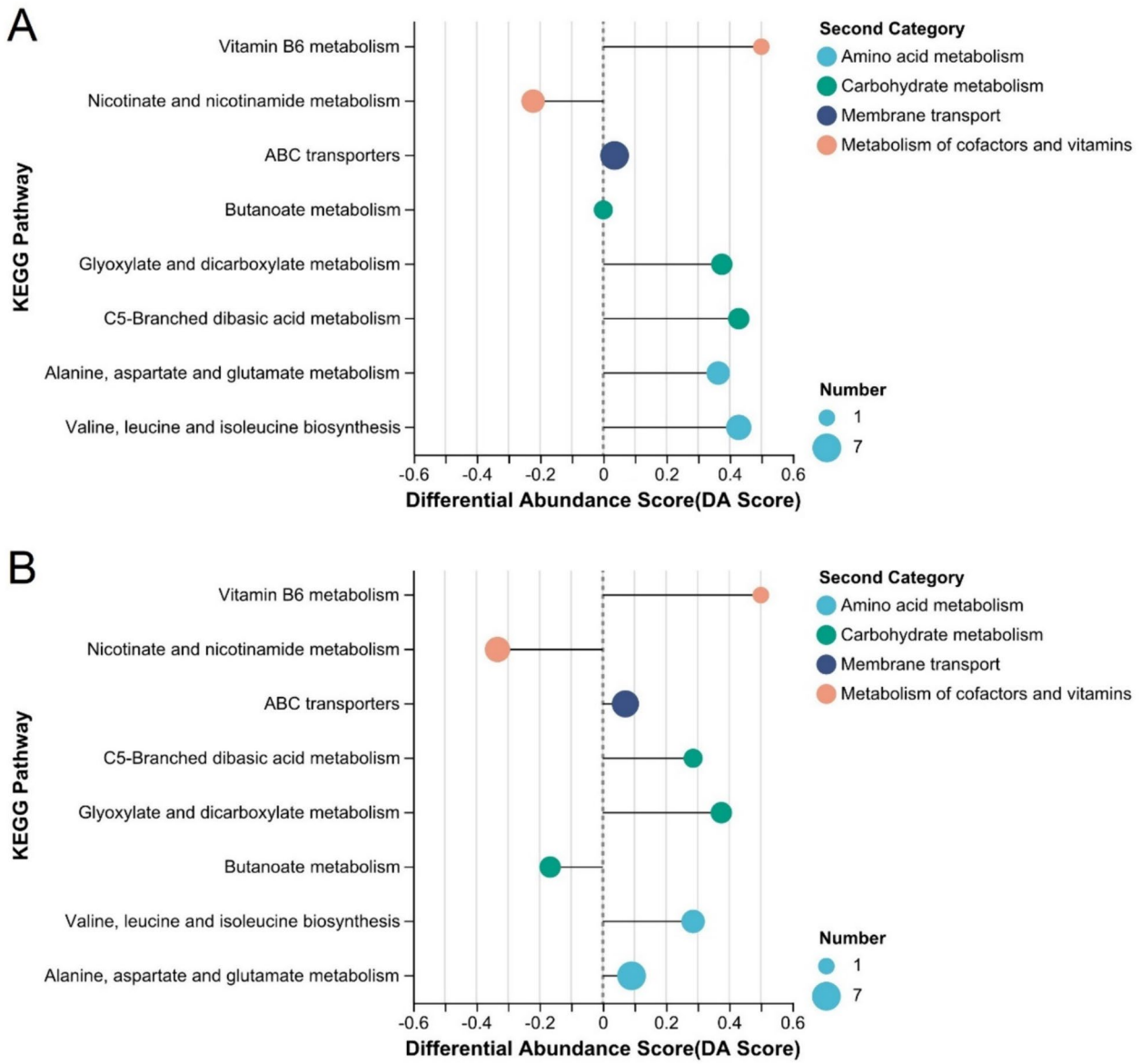

Fig. 6 KEGG Pathway Enrichment Analysis of Differential Metabolites. **A** Between T1 and T2 Treatments; **B** Between T1 and T3 Treatments. T1: control without boron supply; T2: foliar boron supply; T3: root boron supply

greater proportion of ^{10}B in scion tissues following foliar B application compared to root application. This observation implies that foliar application expedites B distribution to scion tissues in pear plants. Notably, B plays a critical role in bud differentiation, leaf extension, and stem tip elongation in pear trees during the post-defoliation stage (Du et al. 2022; Wang et al. 2015). In practice, B is typically supplied through the soil for pear growth after defoliation (Colpaert et al. 2021). However, soil-based B supply often falls short of meeting the demands of pear growth during the post-foliation period when pear trees rely on stem-supported nutrient supply (Neto et al. 2008). The altered B distribution observed with foliar B application suggests its effectiveness as a supplement for restoring stem B levels, advocating for its combined use with soil application during the nutritional recovery phase after pear harvest.

B plays a well-established role in plant growth and yield, with direct and indirect impacts on physiological properties (Diehn et al. 2019; Granado-Rodríguez et al. 2020). Interactions with other mineral nutrients are crucial, with B distribution influencing nutrient status (Saleem et al. 2021). Our study underscores how various B applications affected other mineral nutrients, particularly macro-nutrients N, P, Ca, and Mg, with broader impacts on pear plants. Macro-nutrients exhibit wider healthy ranges in fruit tree tissues compared to micro-nutrients (Han et al. 2009). The pronounced changes

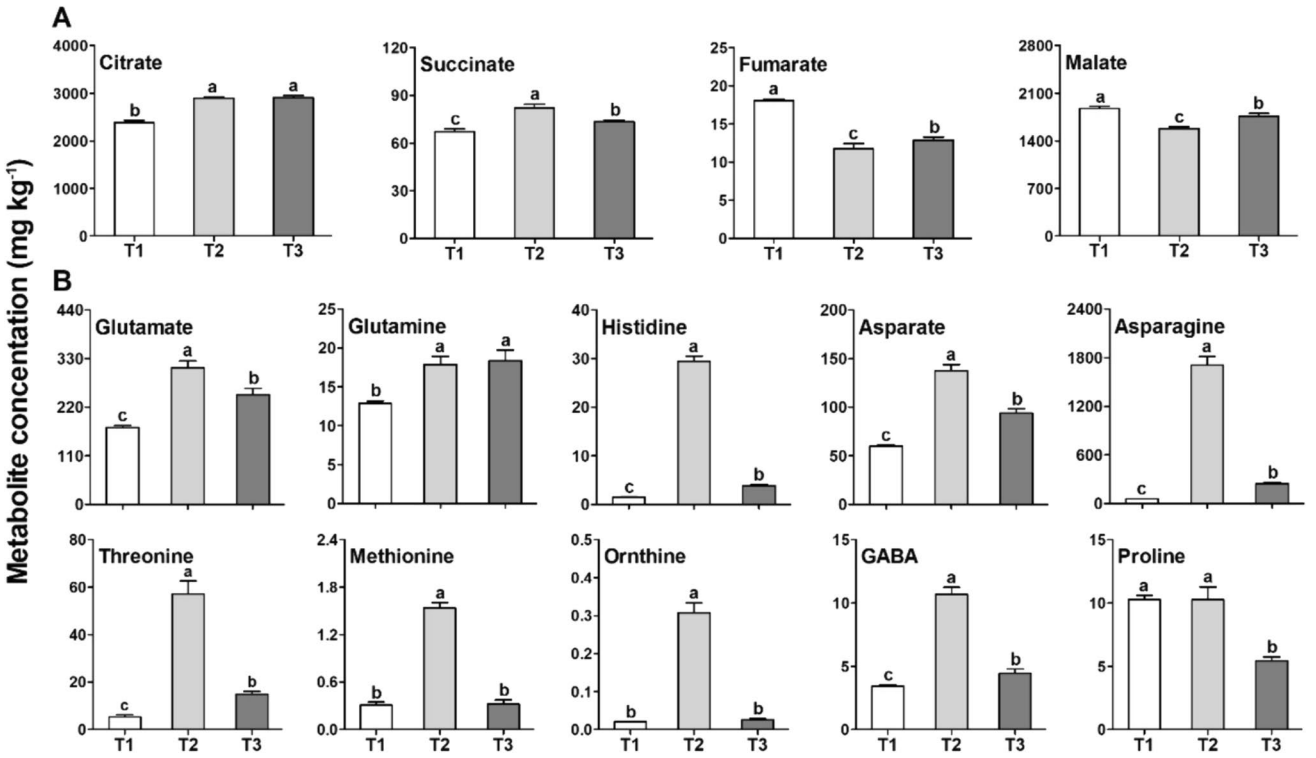

Fig. 7 Comparison of Organic Acid (**A**) and Amino Acid (**B**) Concentration in Leaves of T1-T3 Treated Pear Plants. Different lowercase letters in each graph indicate significant differences among T1-T3 treatments at $P < 0.05$ by Duncan's test. T1: control without boron supply; T2: foliar boron supply; T3: root boron supply. GABA: G Amino Butyric Acid

in macro-nutrient content in response to exogenous B, compared to micro-nutrients (Kohli et al. 2023; Ullah et al. 2012), highlight the susceptibility of macro-nutrient profiles to different B applications. Specifically, N, P, Ca, and Mg are markedly influenced by varying B applications, significantly impacting pear plant growth and nutrient concentration in this study.

It reveals that foliar and root B applications elevate leaf N and Mg concentrations, as well as root Mg concentration, in pear plants. N and Mg are essential for leaf and root growth (Chen et al. 2020; He et al. 2020), suggesting that the observed growth promotion of pear plants is not solely a result of increased B concentration but also linked to improved N and Mg status. Additionally, foliar B application increases Ca concentration in buds and roots while reducing stem Ca concentration, indicating improved Ca absorption and transport capacity from roots to buds in pear plants. Furthermore, foliar B application enhances leaf and stem P concentration, while root B application increases root P concentration, implying that P concentration increases adjacent to the applied B tissues in pear plants.

Different B applications have distinct effects on the distribution of P, Ca, and Mg in pear plants. Foliar application significantly impacts the distribution of leaf P and Mg, while reducing stem P and Ca distribution. Notably, root B application does not differ significantly from the control, suggesting that the distribution of other mineral nutrients is primarily determined by the tissue where B is absorbed in pear plants.

Metabolome analysis of leaves, the primary site of metabolism in pear (Dong et al. 2020), reveals significant changes induced by foliar and root B applications. Differential metabolites, including amino acids, organic acids, fatty acids, and triterpenoids, were prominently altered, indicating close connections between these metabolites and exogenous B supply in pear plants. B concentration directly influences metabolite synthesis and decomposition (Kohli et al. 2023), with increased B concentration driving metabolite pool changes. The upregulation of specific amino acids, organic acids, and fatty acids, intermediates or products of the TCA cycle (Sweetlove et al. 2010), implies that B impacts TCA cycle flux rate, thus modulating carbohydrate metabolism of pear plants. The enhanced carbohydrate metabolism improves plant resistance to stress by providing energy to enhance enzyme activity (Liu et al. 2015). The increased concentration of citrate, a TCA cycle initiator (Sweetlove et al. 2010), following B application, further suggests boosted TCA cycle activity in pear plants. Subsequently, the concentration of GABA and proline (amino acids), the signal or regulator of plant resistance (Liu et al. 2015), was altered

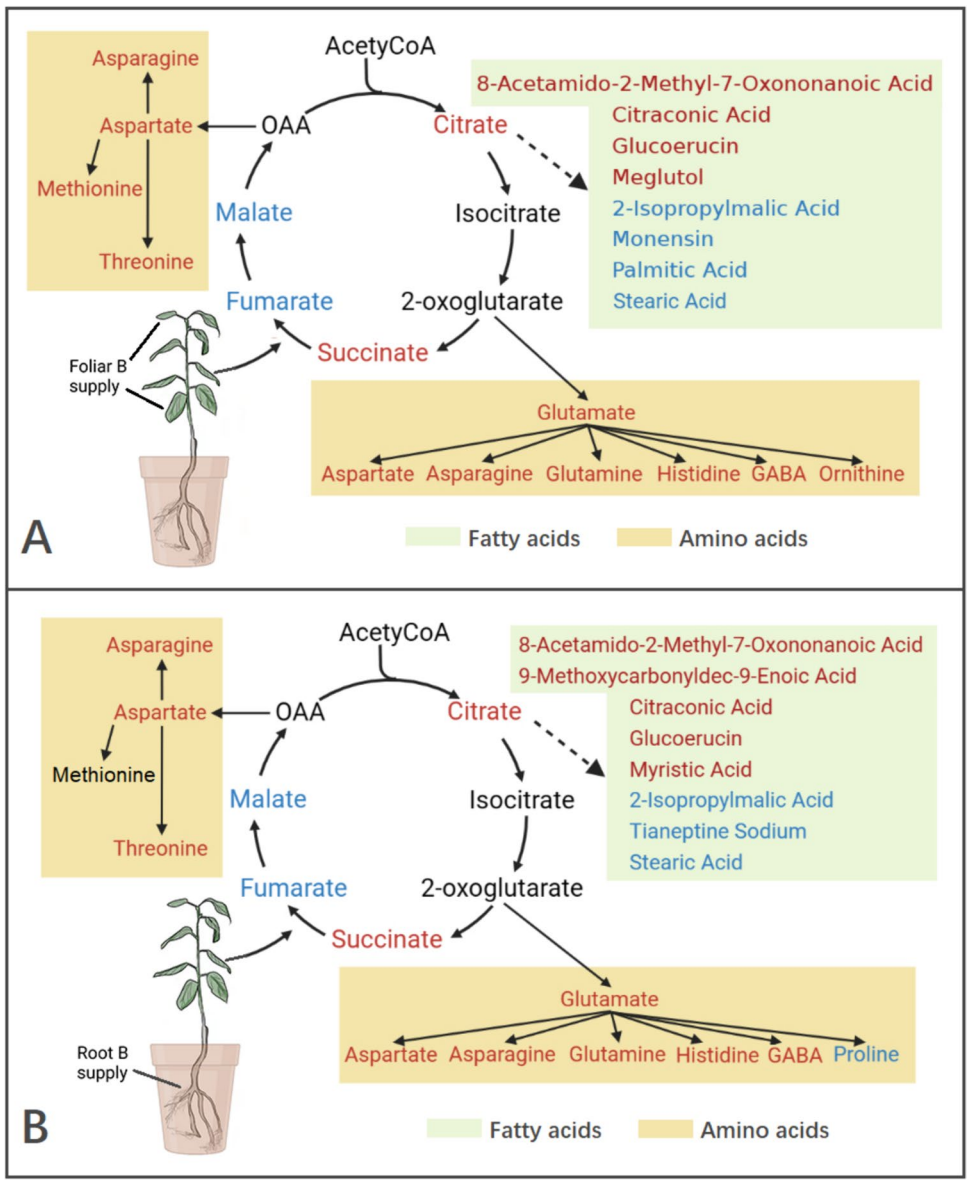

Fig. 8 Schematic Model of Metabolite Changes (Related to the Tricarboxylic Acid Cycle) in Leaves of T1 and T2 (**A**) or T1 and T3 (**B**) Treated Pear Plants. Metabolites with significantly higher levels in T2 and/or T3 treatments than in T1 treatment are highlighted in red font, while metabolites with lower levels are highlighted in blue font. Metabolites displayed in black font indicate no detection in differential metabolites. The significance of difference is calculated by student-*t* test ($P < 0.05$). T1: control without boron supply; T2: foliar boron supply; T3: root boron supply. GABA: G Amino Butyric Acid

after exogenous B supply. Consequently, both foliar and root B applications activate carbohydrate metabolism and amino acid metabolism, enhancing pear plant stress adaptation.

Different B applications affected N, P, Mg concentration in leaves, and influenced TCA cycle resulted in carbohydrate metabolism changes. These effects could play key roles in pear plant resistance. The modulation of N, P, and Mg concentrations in leaves and the subsequent TCA cycle regulation have significant implications for amino acid metabolism and carbohydrate metabolism, essential for plant resistance (Han et al. 2008; Luo et al. 2019; Tegeder and Hammes 2018). Consequently, the modulation of amino acids and fatty acids, which play significant roles in plant resistance (Berestovoy et al. 2020; Liu et al. 2015), can be attributed to increased B content resulting from foliar or root B applications on pear plants.

Elevated leaf N concentration accelerates amino acid metabolism, leading to increased amino acid concentrations (Luo et al. 2020), which are directly related to plant resistance. Furthermore, fatty acids are recognized as key regulators of plant resistance (Berestovoy et al. 2020). The connection between the TCA cycle and fatty acid elongation, facilitated by Mg and P (Berg 1959; Sweetlove et al. 2010), suggests a possible mechanism by which the increased Mg and P concentrations following B application contribute to enhanced resistance through improved fatty acid metabolism in pear plants.

5 Conclusion

This study utilized ^{10}Boron tracing to explore the mechanistic links between boron application methods, boron distribution, nutrient interactions, and metabolic alterations in pear trees. Our findings confirm the efficacy of both foliar and root boron applications in enhancing boron status within pear plants. However, foliar application demonstrates a more rapid and efficient distribution of boron throughout leaves and stems, suggesting its potential as a primary strategy for addressing boron deficiency. The observed impact of boron application methods on the concentrations and distribution of nitrogen, phosphorus, calcium, and magnesium highlights the crucial role of boron in plant mineral nutrient homeostasis. Furthermore, metabolome analysis reveals a predominant influence of boron application methods on carbohydrate and amino acid metabolism pathways in pear leaves. Intriguingly, key metabolic alterations involving amino acids and fatty acids, products of the tricarboxylic acid cycle, suggest a potential role for boron in modulating plant stress responses. This finding warrants further investigation into the precise mechanisms by which boron application enhances pear resistance, potentially through stimulation of the tricarboxylic acid cycle and subsequent changes in leaf metabolite profiles.

Supplementary Information The online version contains supplementary material available at https://doi.org/10.1007/s42729-024-01935-2.

Acknowledgements The authors would like to thank Wang Jia (Shanghai Bioprofile Technologe Company Ltd., Shanghai, China) for his help in data analysis, Chunmei Shi for her help in experimental guidance and Muyao Yang for her help in drawing figures.

Author Contributions Wei Du: Conceptualization, Investigation, Formal analysis, Writing- Original draft preparation, Funding acquisition. Syed Bilal Hussain: Conceptualization, Software, Writing- Reviewing and Editing. Jing Fan: Formal analysis. Qiliang Chen: Formal analysis. Jingguo Zhang: Investigation, Formal analysis. Xiaoping Yang: Conceptualization, Writing- Original draft preparation. Hongju Hu: Conceptualization, Supervision, Funding acquisition.

Funding This study was supported by the National Natural Science Foundation of China (32202420), the Natural Science Foundation of Hubei Province (2023AFB833), the Youth Science Foundation of the Hubei Academy of Agricultural Sciences (2023NKYJJ19) and Hubei Hongshan Laboratory Program (2022hszd009).

Data Availability The data used to support the findings of this study are available from the corresponding author upon request.

Declarations

Conflict of Interest The authors declare no conflicts of interest.

References

Al-Obeed RS, Ahmed MA-A, Kassem HA, Al-Saif AM (2018) Improvement of 'Kinnow' mandarin fruit productivity and quality by urea, boron and zinc foliar spray. J Plant Nutr 41:609–618. https://doi.org/10.1080/01904167.2017.1406111

Archana, Pandey N (2021) Reproductive development and pollen-stigma interaction in sunflower plants receiving boron deficient and toxic supply. J Plant Nutr 44:2157–2166. https://doi.org/10.1080/01904167.2021.1889589

Bairu MW, Stirk WA, Van Staden J (2009) Factors contributing to in vitro shoot-tip necrosis and their physiological interactions. Plant Cell Tissue Org 98:239–248. https://doi.org/10.1007/s11240-009-9560-8

Berestovoy MA, Pavlenko OS, Goldenkova-Pavlova IV (2020) Plant fatty acid desaturases: role in the life of plants and biotechnological potential. Biol Bull Rev 10:127–139. https://doi.org/10.1134/S2079086420020024

Berg P (1959) Role of magnesium in acetyl coenzyme a formation by acetothiokinase. Science 129:895–896. https://doi.org/10.1126/science.129.3353.895

Bolan S, Wijesekara H, Amarasiri D, Zhang T, Ragályi P, Brdar-Jokanović M, Rékási M, Lin J-Y, Padhye LP, Zhao H, Wang L, Rinklebe J, Wang H, Siddique KHM, Kirkham MB, Bolan N (2023) Boron contamination and its risk management in terrestrial and aquatic environmental settings. Sci Total Environ 894:164744. https://doi.org/10.1016/j.scitotenv.2023.164744

Brown PH, Hu H (1996) Phloem mobility of boron is species dependent: evidence for phloem mobility in sorbitol-rich species. Ann Bot 77:497–506. https://doi.org/10.1006/anbo.1996.0060

Chen K-E, Chen H-Y, Tseng C-S, Tsay Y-F (2020) Improving nitrogen use efficiency by manipulating nitrate remobilization in plants. Nat Plants 6:1126–1135. https://doi.org/10.1038/s41477-020-00758-0

Chen Z, Hu Z, Peng J, Sun A, Yan L, Xu Q (2023) Boron isotopic fractionation in Brassica napus L. plants during plant growth under hydroponic conditions. Plant Soil 485:411–423. https://doi.org/10.1007/s11104-022-05839-x

Colpaert B, Steppe K, Gomand A, Vanhoutte B, Remy S, Boeckx P (2021) Experimental approach to assess fertilizer nitrogen use, distribution, and loss in pear fruit trees. Plant Physiol Biochem 165:207–216. https://doi.org/10.1016/j.plaphy.2021.05.019

Diehn TA, Bienert MD, Pommerrenig B, Liu Z, Spitzer C, Bernhardt N, Fuge J, Bieber A, Richet N, Chaumont F, Bienert GP (2019) Boron demanding tissues of Brassica napus express specific sets of functional Nodulin26-like Intrinsic Proteins and BOR1 transporters. Plant J 100:68–82. https://doi.org/10.1111/tpj.14428

Dong X, Wang Z, Tian L, Zhang Y, Qi D, Huo H, Xu J, Li Z, Liao R, Shi M, Wahocho SA, Liu C, Zhang S, Tian Z, Cao Y (2020) De novo assembly of a wild pear (*Pyrus betuleafolia*) genome. Plant Biotechnol J 18:581–595. https://doi.org/10.1111/pbi.13226

Du W, Shi C, Hussain SB, Li M, Fan J, Chen Q, Zhang J, Liu Y, Yang X, Hu H (2022) Morpho-physiological and transcriptome analyses provide insights into the wizened bud formation in pear trees. Agronomy 12:484. https://doi.org/10.3390/agronomy12020484

Fernández V, Eichert T (2009) Uptake of hydrophilic solutes through plant leaves: current state of knowledge and perspectives of foliar fertilization. Crit Rev Plant Sci 28:36–68. https://doi.org/10.1080/07352680902743069

Gao Y-Q, Chao D-Y (2022) Localization and circulation: vesicle trafficking in regulating plant nutrient homeostasis. Plant J 112:1350–1363. https://doi.org/10.1111/tpj.16020

García-Sánchez F, Simón-Grao S, Martínez-Nicolás JJ, Alfosea-Simón M, Liu C, Chatzissavvidis C, Pérez-Pérez JG, Cámara-Zapata JM (2020) Multiple stresses occurring with boron toxicity and deficiency in plants. J Hazard Mater 397:122713. https://doi.org/10.1016/j.jhazmat.2020.122713

Granado-Rodríguez S, Bolaños L, Reguera M (2020) *MtNIP5;1*, a novel *Medicago truncatula* boron diffusion facilitator induced under deficiency. BMC Plant Biol 20:552. https://doi.org/10.1186/s12870-020-02750-4

Han S, Chen L-S, Jiang H-X, Smith BR, Yang L-T, Xie C-Y (2008) Boron deficiency decreases growth and photosynthesis, and increases starch and hexoses in leaves of citrus seedlings. J Plant Physiol 165:1331–1341. https://doi.org/10.1016/j.jplph.2007.11.002

Han S, Tang N, Jiang H-X, Yang L-T, Li Y, Chen L-S (2009) CO_2 assimilation, photosystem II photochemistry, carbohydrate metabolism and antioxidant system of citrus leaves in response to boron stress. Plant Sci 176:143–153. https://doi.org/10.1016/j.plantsci.2008.10.004

He H, Jin X, Ma H, Deng Y, Huang J, Yin L (2020) Changes of plant biomass partitioning, tissue nutrients and carbohydrates status in magnesium-deficient banana seedlings and remedy potential by foliar application of magnesium. Sci Hortic 268:109377. https://doi.org/10.1016/j.scienta.2020.109377

Jiang H-b, Li H-x, Zhao M-x, Mei X-l, Kang Y-l, Dong C-x, Xu Y (2020) Strategies for timing nitrogen fertilization of pear trees based on the distribution, storage, and remobilization of ^{15}N from seasonal application of $(^{15}NH_4)_2SO_4$. J Integr Agric 19:1340–1353. https://doi.org/10.1016/S2095-3119(19)62758-9

Kohli SK, Kaur H, Khanna K, Handa N, Bhardwaj R, Rinklebe J, Ahmad P (2023) Boron in plants: uptake, deficiency and biological potential. Plant Growth Regul 100:267–282. https://doi.org/10.1007/s10725-022-00844-7

Landi M, Margaritopoulou T, Papadakis IE, Araniti F (2019) Boron toxicity in higher plants: an update. Planta 250:1011–1032. https://doi.org/10.1007/s00425-019-03220-4

Liu G, Dong X, Liu L, Wu L, Sa P, Jiang C (2015) Metabolic profiling reveals altered pattern of central metabolism in navel orange plants as a result of boron deficiency. Physiol Plant 153:513–524. https://doi.org/10.1111/ppl.12279

Liu J, Chen T, Wang C-L, Liu X (2023) Transcriptome analysis in *Pyrus betulaefolia* roots in response to short-term boron deficiency. Genes 14:817. https://doi.org/10.3390/genes14040817

López-Lefebre LR, Rivero RM, García PC, Sánchez E, Ruiz JM, Romero L (2002) Boron effect on mineral nutrients of tobacco. J Plant Nutr 25:509–522. https://doi.org/10.1081/PLN-120003379

Lu Y-B, Yang L-T, Li Y, Xu J, Liao T-T, Chen Y-B, Chen L-S (2014) Effects of boron deficiency on major metabolites, key enzymes and gas exchange in leaves and roots of Citrus sinensis seedlings. Tree Physiol 34:608–618. https://doi.org/10.1093/treephys/tpu047

Luo B, Ma P, Nie Z, Zhang X, He X, Ding X, Feng X, Lu Q, Ren Z, Lin H, Wu Y, Shen Y, Zhang S, Wu L, Liu D, Pan G, Rong T, Gao S (2019) Metabolite profiling and genome-wide association studies reveal response mechanisms of phosphorus deficiency in maize seedling. Plant J 97:947–969. https://doi.org/10.1111/tpj.14160

Luo L, Zhang Y, Xu G (2020) How does nitrogen shape plant architecture? J Exp Bot 71:4415–4427. https://doi.org/10.1093/jxb/eraa187

Mahendran PP, Suganya S, Kannan P, Yuvaraj M (2022) Growth, nutrient uptake, yield and quality parameters of nendran banana (*Musa spp.*): as influenced by the application of boron in typic rhodustalf of Theni district, Tamil Nadu, India. Commun Soil Sci Plant Anal 53:559–575. https://doi.org/10.1080/00103624.2021.2017958

Matthes MS, Robil JM, McSteen P (2020) From element to development: the power of the essential micronutrient boron to shape morphological processes in plants. J Exp Bot 71:1681–1693. https://doi.org/10.1093/jxb/eraa042

Neto C, Carranca C, Clemente J, de Varennes A (2008) Nitrogen distribution, remobilization and re-cycling in young orchard of non-bearing 'Rocha' pear trees. Sci Hortic 118:299–307. https://doi.org/10.1016/j.scienta.2008.06.023

Pawlowski ML, Helfenstein J, Frossard E, Hartman GL (2019) Boron and zinc deficiencies and toxicities and their interactions with other nutrients in soybean roots, leaves, and seeds. J Plant Nutr 42:634–649. https://doi.org/10.1080/01904167.2019.1567782

Pereira GL, Siqueira JA, Batista-Silva W, Cardoso FB, Nunes-Nesi A, Araújo WL (2021) Boron: more than an essential element for land plants? Front Plant Sci 11:610307. https://doi.org/10.3389/fpls.2020.610307

Saleem MH, Wang X, Ali S, Zafar S, Nawaz M, Adnan M, Fahad S, Shah A, Alyemeni MN, Hefft DI, Ali S (2021) Interactive effects of gibberellic acid and NPK on morpho-physio-biochemical traits and organic acid exudation pattern in coriander (*Coriandrum sativum* L.) grown in soil artificially spiked with boron. Plant Physiol Biochem 167:884–900. https://doi.org/10.1016/j.plaphy.2021.09.015

Shireen F, Nawaz MA, Chen C, Zhang Q, Zheng Z, Sohail H, Sun J, Cao H, Huang Y, Bie Z (2018) Boron: functions and approaches to enhance its availability in plants for sustainable agriculture. Int J Mol Sci 19:1856. https://doi.org/10.3390/ijms19071856

Silva G, Souza TM, Barbieri RL, Costa de Oliveira A (2014) Origin, domestication, and dispersing of pear (*Pyrus spp.*). Adv Agron 2014:541097. https://doi.org/10.1155/2014/541097

Sweetlove LJ, Beard KFM, Nunes-Nesi A, Fernie AR, Ratcliffe RG (2010) Not just a circle: flux modes in the plant TCA cycle. Trends Plant Sci 15:462–470. https://doi.org/10.1016/j.tplants.2010.05.006

Tegeder M, Hammes UZ (2018) The way out and in: phloem loading and unloading of amino acids. Curr Opin Plant Biol 43:16–21. https://doi.org/10.1016/j.pbi.2017.12.002

Tian XY, He DD, Bai S, Zeng WZ, Wang Z, Wang M, Wu LQ, Chen ZC (2021) Physiological and molecular advances in magnesium nutrition of plants. Plant Soil 468:1–17. https://doi.org/10.1007/s11104-021-05139-w

Tian J, Lu X, Chen Q, Kuang X, Liang C, Deng L, Lin D, Cai K, Tian J (2022) Phosphorus fertilization affects soybean rhizosphere phosphorus dynamics and the bacterial community in karst soils. Plant Soil:1–16. https://doi.org/10.1007/s11104-020-04662-6

Ullah S, Khan AS, Malik AU, Afzal I, Shahid M, Razzaq K (2012) Foliar application of boron influences the leaf mineral status, vegetative and reproductive growth, yield and fruit quality of 'kinnow' mandarin (*Citrus reticulata* blanco.). J Plant Nutr 35:2067–2079. https://doi.org/10.1080/01904167.2012.717661

Wang N, Yang C, Pan Z, Liu Y, Sa Peng (2015) Boron deficiency in woody plants: various responses and tolerance mechanisms. Front Plant Sci 6:128665. https://doi.org/10.3389/fpls.2015.00916

Wang Y, Zhao Z, Wang S, Shi L, Ding G, Xu F (2022) Boron mediates nitrogen starvation-induced leaf senescence by regulating ROS production and C/N balance in Brassica napus. Environ Exp Bot 200:104905. https://doi.org/10.1016/j.envexpbot.2022.104905

Wang J, Li H, Wang Q, Huang X, Hu W, Wang S, Zhou Z (2023) Effects of phosphorus application on carbohydrate metabolism in cottonseed kernel during the key development period provided a new insight for phosphorus management in cotton production. Ind Crops Prod 191:115972. https://doi.org/10.1016/j.indcrop.2022.115972

Xuan H, Streif A, Römheld V, Bangerth F (2005) Application of boron with calcium affects respiration and ATP/ADP ratio in 'Conference' pears during controlled atmosphere storage. J Hortic Sci Biotech 80:633–637. https://doi.org/10.1080/14620316.2005.11511990

Zhang Q, Ackah M, Wang M, Amoako FK, Shi Y, Wang L, Dari L, Li J, Jin X, Jiang Z, Zhao W (2023) The impact of boron nutrient supply in mulberry (*Morus alba*) response to metabolomics, enzyme activities, and physiological parameters. Plant Physiol Biochem 200:107649. https://doi.org/10.1016/j.plaphy.2023.107649

Zhao D, Oosterhuis DM (2002) Cotton carbon exchange, nonstructural carbohydrates, and boron distribution in tissues during development of boron deficiency. Field Crop Res 78:75–87. https://doi.org/10.1016/S0378-4290(02)00095-3

Zhou GF, Peng SA, Liu YZ, Wei QJ, Han J, Islam MZ (2014) The physiological and nutritional responses of seven different citrus rootstock seedlings to boron deficiency. Trees 28:295–307. https://doi.org/10.1007/s00468-013-094